

Article

Energy Analysis and Multi-Objective Optimization of an Internal Combustion Engine-Based CHP System for Heat Recovery

Abdolsaeid Ganjehkaviri *and Mohammad Nazri Mohd Jaafar

Faculty of Mechanical Engineering, Universiti Teknologi Malaysia, 81310 UTM Skudai, JB, Malaysia; E-Mail: nazrii@mail.fkm.utm.my

* Author to whom correspondence should be addressed; E-Mail: s.ganjehkaviri@gmail.com; Tel.: +6010-7017576.

External Editor: Marc A. Rosen

Received: 18 July 2014; in revised form: 1 September 2014 / Accepted: 16 October 2014 /

Published: 27 October 2014

Abstract: A comprehensive thermodynamic study is conducted of a diesel based Combined Heat and Power (CHP) system, based on a diesel engine and an Organic Rankine Cycle (ORC). Present research covers both energy and exergy analyses along with a multi-objective optimization. In order to determine the irreversibilities in each component of the CHP system and assess the system performance, a complete parametric study is performed to investigate the effects of major design parameters and operating conditions on the system's performance. The main contribution of the current research study is to conduct both exergy and multi-objective optimization of a system using different working fluid for low-grade heat recovery. In order to conduct the evolutionary based optimization, two objective functions are considered in the optimization; namely the system exergy efficiency, and the total cost rate of the system, which is a combination of the cost associated with environmental impact and the purchase cost of each component. Therefore, in the optimization approach, the overall cycle exergy efficiency is maximized satisfying several constraints while the total cost rate of the system is minimized. To provide a better understanding of the system under study, the Pareto frontier is shown for multi-objective optimization and also an equation is derived to fit the optimized point. In addition, a closed form relationship between exergy efficiency and total cost rate is derived.

Keywords: diesel engine; optimization; exergy analysis; organic Rankine cycle

1. Introduction

Efficiency improvement of energy systems has been a focus among researchers and designers during the last few decades. Thermal power plants have become more common in many power production sites around the world. These industries are forced to enhance their technologies and use more green options and high efficient cycles. One of the potential options to increase the efficiency of such systems is energy integration that can utilize waste heat to produce useful output, *i.e.*, electricity, heating, cooling and even hot water.

Among different kinds of energy recovery systems, Organic Rankine Cycles (ORC) have gained a lot of attention due to their use of low-grade heat waste from exhaust gas and coolant in an internal combustion engine (ICE) [1–4]. For instance, a Spark Ignition with 1.4 L ICE and thermal efficiency of 15–32%, wastes 1.7–45 kW of energy through radiator coolant and 4.6–120 kW of through exhaust gas [5]. During the past decades, many researchers have conducted different configurations of Rankine Cycles by using different working fluids to improve the systems' performance [6–15]. Papadopoulos *et al.* [16] investigated the first approach to the systematic design and the selection of optimal working fluids for Organic Rankine Cycles based on CAMD (computer aided molecular design) and process optimization techniques. Wakui *et al.* [17] studied optimal sizing of the residential gas engine cogeneration system for the power interchange operation from an energy saving viewpoint by conducting optimal operational planning based on mixed-integer linear programming. They concluded that energy savings increase with system scale, as the heat to power ratio of the system decreases and approached that of demand due to the increase in efficiency generated. Alanne *et al.* [18] conducted a study to determine optimal strategies for the integration of a sterling engine based micro cogeneration system in residential buildings by comparing the performance of various system configurations and operational strategies with that of a reference system, *i.e.* hydraulic heating and a low temperature gas boiler in standard and passive house constructions located in different climates. They suggested that an optimally operated micro-cogeneration system encompassing heat recovery and appropriate thermal storage would result in 3–5% decrease in primary energy consumption and CO₂ emissions when compared with a conventional hydraulic heating system. Ren *et al.* [19] investigated two typical micro CHP alternatives, namely, gas engine and fuel cell for residential buildings. For each facility, two different operating modes including minimum-cost operation and minimum-emission operation were taken into consideration by employing a plan and evaluation model for residential micro combined heat and power (CHP) systems. Aussant *et al.* [20] modeled a group of test case houses using a high resolution building simulation program to evaluate the efficiency of an internal combustion engine (ICE) to determine the economical (in terms of fuel cost) impact of using ICE. The performance—in terms of electrical and CHP efficiencies—of the ICE-based cogeneration systems in Canada was investigated and it was determined that the performance of the ICE-based cogeneration system depended on the thermal and electrical loads of the house, especially the severity and duration of the heating season. In this regard, the following steps were undertaken:

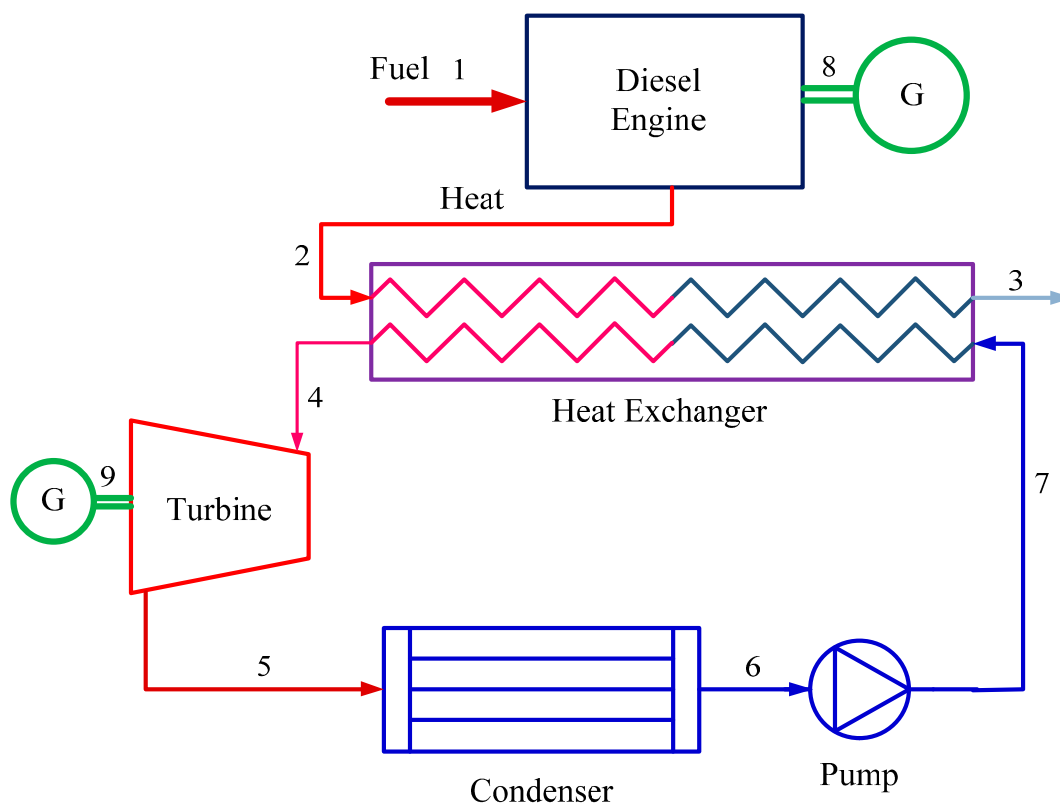
- Model the diesel based CHP system
- Perform energy and exergy analyses and an environmental impact assessment of the system
- Determine the exergy efficiency and exergy destruction rate of each component
- Apply an optimization technique based on a code developed in the Matlab software
- Propose a new closed-form expression relating the exergy efficiency and total cost rate

- Develop an equation for the Pareto optimal points curve to provide an aid for the optimal design of the multi-generation plant

2. System Description

The schematic of the cogeneration system based on ICE is shown in Figure 1. The Caterpillar G3306B, ICE with a nominal power output of 125 kW is considered in this study, which consumes natural gas as its fuel. The engine is connected to an electrical generator to produce electrical power and also heat exchangers at the water jackets and exhaust gas for the heat recovery. The rejected heat from the diesel engine is utilized as the energy input to the Organic Rankine Cycle (ORC) to produce electricity. The output temperature of the hot water and diesel gases are varied due to the partial load, and other parameters of the engine are varied. The waste heat from the ORC is then utilized to produce steam in the heating process via the heat exchanger. The high pressure and high temperature vapor at point 4 is expanded through a turbine to generate power, and vapor extracted from the turbine enters the condenser for the heating process. The saturated liquid exits the condenser and enters the ORC pump at point 6. The ORC pump increases the pressure of ORC working fluid, and high pressure ORC fluid enters the ORC evaporator at point 7 to complete the ORC power generation unit.

Figure 1. Schematic of diesel engine based Combined Heat and Power (CHP) system.



3. Modeling and Energy Analysis

To model the present CHP system, a simulation computer code using Matlab software was developed. The two main parts of the CHP system as mentioned before (ORC and diesel engine) are first individually modeled to include exergy flow rate. Engineering equation solver (EES) is linked to Matlab in order to calculate the properties (e.g., pressure, temperature, enthalpy and entropy) of the different working fluids. Several simplifying assumptions are made here to render the analysis more tractable, while retaining adequate accuracy to illustrate the principal points of the study:

- All processes operate at steady state
- The condenser outlet state is a saturated liquid, and its temperature is assumed to be approximately 5 °C higher than the environment temperature
- The working fluid at the evaporator outlet is a saturated vapor
- The pressure drop in the ORC cycle is negligible
- The heat loss from piping and other auxiliary components is negligible

According to the advances in the design of compact heat exchangers, temperature differences between inlet air and condenser outlet for cross flow configuration can reach values lower than 10 °C and close to 5 °C [21]. For thermodynamic modeling, the CHP system considered here (Figure 1) is divided into two main sub-systems: (1) diesel engine and, (2) Organic Rankine Cycle. By applying energy analysis, the temperature profile, input and output enthalpies of this CHP plant are determined. By applying the exergy analysis, the exergy flows, exergy efficiencies and exergy destruction rate of the plant can be determined. The relevant energy balances of the plant are described below.

3.1. Diesel Engine

A diesel engine—also known as a compression ignition engine—is an internal combustion engine that uses the heat of compression to initiate ignition and burn the fuel that has been injected into the combustion chamber.

In diesel engines, the heat lost to water jacket and exhaust can be recovered and utilized to produce either heat or power in another cycle. Diesel engine characteristics such as thermal efficiency, power production and recoverable heat are a function of partial load defined as the percentage of nominal load. It is obvious that an increase in partial load results in an increase in both power and heat production which eventually leads to an increase in mass flow rate injected into the engine. Therefore, the optimal partial load should be determined in order to optimize the system. There are several methods to calculate the output power and heat production from diesel engine as a function of partial load, however we have used the relation used in [9]. The power generated by a diesel engine can be expressed as:

$$\frac{\dot{W}_{Die,PL}}{\dot{m}_{f,PL}LHV_f} = \{1.07 \exp(-0.000574(PL)) - 1.26 \exp(-0.0537(PL))\eta_{D,nom}\} \quad (1)$$

where LHV_f is the fuel lower heating value (47,828 kJ/kg in this study), PL the partial load and $\eta_{D,nom}$ is diesel engine nominal efficiency.

Recoverable energy from the water jacket and exhaust gas enthalpy as a function of partial load are expressible as:

$$\frac{\dot{Q}_{wj,PL}}{\dot{m}_{f,PL}LHV_f} = 24.01 \exp(-0.0248(PL)) + 15.35 \exp(0.00282(PL)) \quad (2)$$

$$\frac{\dot{Q}_{o,PL}}{\dot{m}_{f,PL}LHV_f} = (0.001016(PL)^2 - 0.1423(PL) + 31.72) \quad (3)$$

In addition, un-recoverable energy from oil and other components as a function of partial load can be expressed as follows:

$$\frac{\dot{Q}_{oil,PL}}{\dot{m}_{f,PL}LHV_f} = 1.33 \times 10^{-7}(PL)^4 - 4.35 \times 10^{-5}(PL)^3 + 0.0056(PL)^2 - 0.107(PL) + 15.64. \quad (4)$$

$$\frac{\dot{Q}_{Others,PL}}{\dot{m}_{f,PL}LHV_f} = \{-3.26 \times 10^{-6}(PL)^3 + 0.0013(PL)^2 - 0.106PL + 15.64\} \quad (5)$$

3.2. ORC Cycle

The ORC cycle here has the following four main components:

- Heat Exchanger (evaporator)

The temperature profile and enthalpy of flows through the ORC evaporator are modelled as follows. While the configuration details of the heat exchanger can be found in [22], the following energy balance can be applied to the evaporator:

$$\dot{Q} = \dot{m}_4 h_4 - \dot{m}_7 h_7 \quad (6)$$

- ORC Turbine

The energy balance of the ORC turbine is written as follow:

$$\dot{m}_4 h_4 = \dot{W}_T + \dot{m}_5 h_5 \quad (7)$$

Also, the isentropic efficiency of the turbine becomes

$$\eta_{ORC,T} = \frac{\dot{W}_{ORC,act}}{\dot{W}_{ORC,is}} \quad (8)$$

where h_4 and h_5 are the inlet and outlet enthalpies and $\dot{W}_{ORC,act}$ and $\dot{W}_{ORC,is}$ are actual and isentropic turbine power outputs.

- ORC Condenser

The energy balance of the ORC condenser is as follow:

$$\dot{m}_5 h_5 = \dot{m}_6 h_6 + \dot{Q}_{Cond} \quad (9)$$

- ORC Pump

The energy balance of the ORC pump is written as follow:

$$\dot{W}_{ORC,p} = \dot{m}_6(h_7 - h_6) \quad (10)$$

4. Exergy Analysis

Unlike energy, exergy is a measure of the quality of energy that can be considered to evaluate, analyze and optimize the system. Exergy analysis is utilized to define the maximum performance of a system and to specify its irreversibilities [23–25]. Combining the first and second law of thermodynamics, the following exergy rate balance is derived as:

$$\dot{E}x_Q + \sum_i \dot{m}_i ex_i = \sum_e \dot{m}_e ex_e + \dot{E}x_W + \dot{E}x_D \quad (11)$$

where subscripts i and e denote the control volume inlet and outlet flow, respectively, $\dot{E}x_D$ is the exergy destruction rate and other terms are given as follows:

$$\dot{E}x_Q = (1 - \frac{T_0}{T_i})\dot{Q}_i; \dot{E}x_w = \dot{W}; ex = ex_{ph} + ex_{ch} \quad (12)$$

Here, $\dot{E}x_Q$ is the exergy rate of heat transfer crossing the boundary of the control volume at absolute temperature T , the subscript 0 refers to the reference environment conditions and $\dot{E}x_W$ is the exergy rate associated with shaft work. Also, ex_{ph} is defined as follows:

$$ex_{ph} = (h - h_0) - T_0(s - s_0) \quad (13)$$

The chemical exergy can be written as follows [26]:

$$ex_{mix}^{ch} = [\sum_{i=1}^n x_i ex_i^{ch} + RT_0 \sum_{i=1}^n x_i \ln x_i] \quad (14)$$

Here, the exergy of each flow is calculated at all states and the changes in exergy are determined for each major component. The exergy destructions for all components in CHP system (Figure 1) are listed in Table 1. The exergy efficiency, defined as the product exergy output divided by the exergy input [26], can be expressed for the CHP system as follows:

$$\psi = \frac{\dot{W}_{Die} + \dot{W}_T - \dot{W}_P}{\dot{E}x_f} \quad (15)$$

where \dot{W}_{Die} , \dot{W}_T and \dot{W}_P are diesel engine work, ORC turbine shaft work and pumping work respectively. $\dot{E}x_f$ is fuel chemical exergy.

Table 1. The exergy destruction equations for each component.

Components	Exergy Destruction
Diesel	$\dot{E}x_{D,Die} = \dot{E}x_{Fuel} - \dot{E}x_{Q,HEX} - \dot{W}_{Die}$
Heat exchanger	$\dot{E}x_{D,HEX} = (\dot{E}x_2 + \dot{E}x_7) - (\dot{E}x_3 + \dot{E}x_4)$
Turbine	$\dot{E}x_{D,T} = \dot{E}x_4 - \dot{E}x_9 - \dot{W}_T$
Condenser	$\dot{E}x_{D,Cond} = \dot{E}x_5 - \dot{E}x_6 - \dot{E}x_{Q,Cond}$
Pump	$\dot{E}x_{D,P} = \dot{E}x_6 - \dot{E}x_7 + \dot{W}_P$

5. Multi-Objective Optimization

To find the best design parameters for the system, a multi-objective optimization method based on an evolutionary algorithm is applied. Therefore, the definition of objective functions, design parameters and constraints, and optimization are represented as follow.

5.1. Definition of Objectives

In this research study, two different objective functions which are exergy efficiency (to be maximized) and total product cost rate (to be minimized) are considered.

Pollution damage cost is added directly to the expenditures that must be paid. Therefore, the objective functions in this analysis are written below:

(1) Exergy Efficiency

First objective function is selected as the exergy efficiency of the cycle. The calculation of exergy efficiency is shown in Equation (15).

(2) Total Cost Rate

$$\dot{C}_{tot} = \sum_k \dot{Z}_k + \dot{C}_f + \dot{C}_{env} \tag{16}$$

where the fuel cost and the cost rates of environmental impact are display as:

$$\dot{C}_f = c_f \dot{m}_f LHV_f \ \& \ \dot{C}_{env} = C_{CO_2} \dot{m}_{CO_2} \tag{17}$$

Here, \dot{Z}_k is the purchase cost of each component. Purchase cost functions of each equipment are listed in Table 2 [3,27,28]. c_f is the diesel fuel cost which is 0.168 \$/kg in our study. In this analysis, we express the environmental impact as the total cost rate of pollution damage (\$/s) due to CO₂ emissions by multiplying their respective flow rates by their corresponding unit damage costs (C_{CO_2} is taken to be 0.024 \$/kg) [3]. The cost of pollution damage is assumed to be added directly to other system costs.

Table 2. Purchase cost functions of each equipment.

Components	Exergy Destruction
Diesel*	$\dot{Z}_{Die} = \left[\frac{-138.71}{2} \times \ln(Enom_{turbine}) + 1727.1 \right] \times Enom_{turbine}$
Turbine	$\dot{Z}_T = 4750 \times \dot{W}_T^{0.75}$
Condenser	$\dot{Z}_{Cond} = 150 \times A_{Cond}^{0.8}$
Pump	$\dot{Z}_P = 3500 \times \dot{W}_P^{0.45}$

*: heat exchanger cost has been considered in diesel engine cost.

5.2. Decision Variables

The following decision variables are selected for the study: diesel engine nominal power (\dot{W}_{Nom}), diesel engine partial load (PL), ORC turbine inlet pressure (P_4), ORC condenser pressure (P_5), ORC turbine isentropic efficiency (η_T), ORC pump isentropic efficiency (η_p). In addition, due to the modeling and objective function developing algorithm, the engine size is determined exactly by the selected decision variables. Although the decision variables may be varied in the optimization procedure, each is required to be within a reasonable range. Such constraints, based on earlier reports, are listed in Table 3 [26].

Table 3. Optimization constraints and their rationales.

Constraint	Reason
$50 \text{ kW} < \dot{W}_{Nom} < 200 \text{ kW}$	Diesel engine size limitation
$50 < PL < 100$	Diesel engine load limitation
$1000 \text{ kPa} < P_{main} < 2500 \text{ kPa}$	Commercial availability
$50 \text{ kPa} < P_{Cond} < 300 \text{ kPa}$	Commercial availability
$\eta_T < 0.9$	Commercial availability
$\eta_p < 0.9$	Commercial availability

5.3. Evolutionary Algorithm: Genetic Algorithm

Of the many optimization techniques known, evolutionary algorithm (EA) is known as one the most important, as a set of modern-met heuristics used successfully in many applications with great complexity. Evolutionary algorithms are highly connected by industrial applications due to their capability of solving problems with multiple objectives, nonlinear constraints and dynamic components properties which frequently appear in real problems. To find a global optimum a global, robust and efficient method is needed. The specifications of the problem along with many literature citations propose EA optimization as a useful, trustable and direct method [29,30].

6. Results and Discussion

6.1. Working Fluid Selection

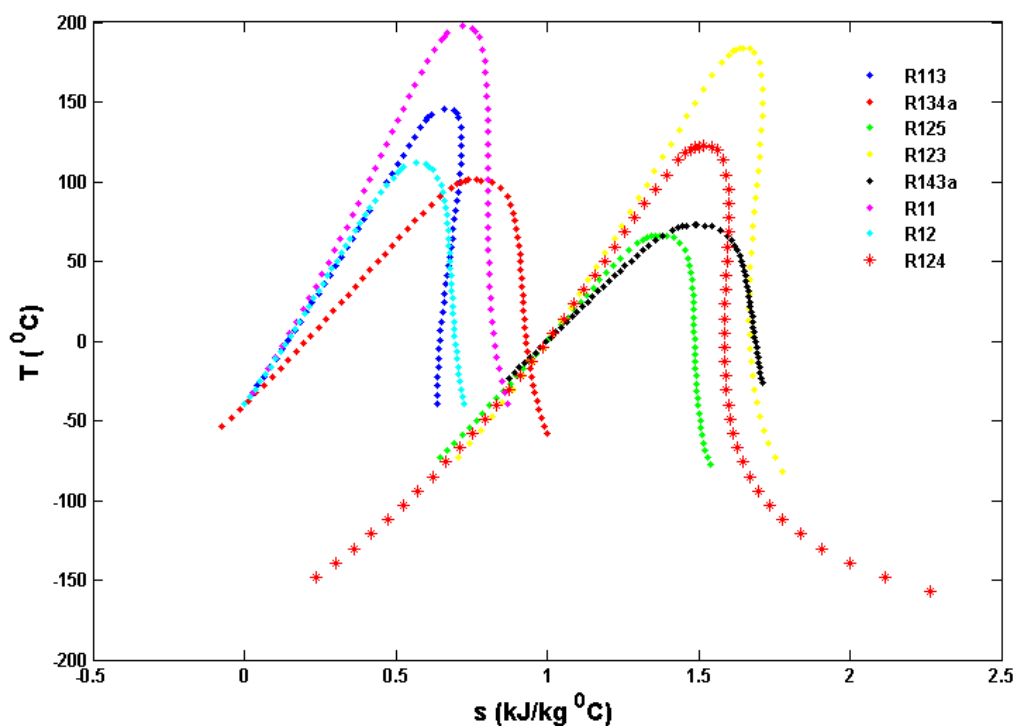
Various working fluids usually can be classified into three categories according to the slope of the saturation vapor line in a T-s diagram. In this study, performance assessments of different working fluids are conducted to see the effect of the different fluids on exergy efficiency of the diesel engine CHP system. The T-s diagram of different working fluids for this study is shown in Figure 2. The thermo physical properties of the selected working fluids are listed in Table 4.

Table 4. The thermo physical properties of the selected working fluids.

Number	Substance	Molecular mass [kg/kmol]	T_b^a (K)	P_{cr}^b (MPa)	T_{cr}^a (K)
1	R123	152.93	300.97	3.66	456.83
2	R134a	102.03	247.08	4.059	374.21
3	R124	136.48	261.22	3.62	395.43
4	R11	137.37	296.86	4.40	471.11
5	R12	120.91	243.4	4.13	385.12
6	R143a	84.04	161.34	3.76	345.86
7	R113	187.38	320.74	3.39	487.21
8	R125	120.02	172.52	3.61	339.17
9	R141b	116.95	305.2	4.46	479.96

T_b^a : Normal boiling point; P_{cr}^b : Critical pressure; T_{cr}^a : Critical temperature.

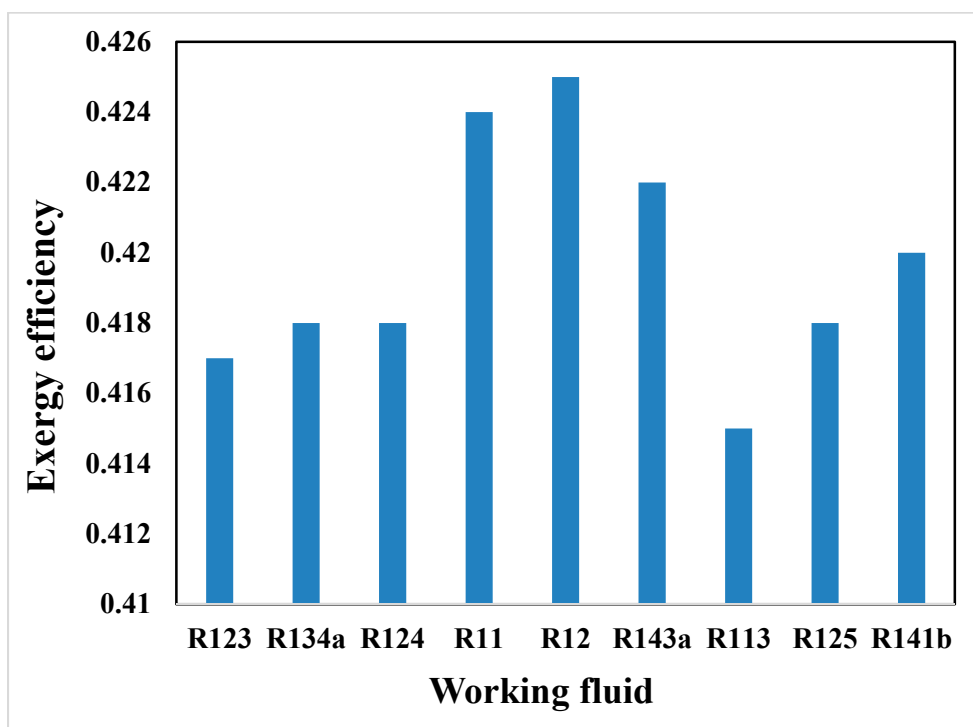
Figure 2. T-s diagram of selected working fluids.



6.2. Exergy Analysis Results

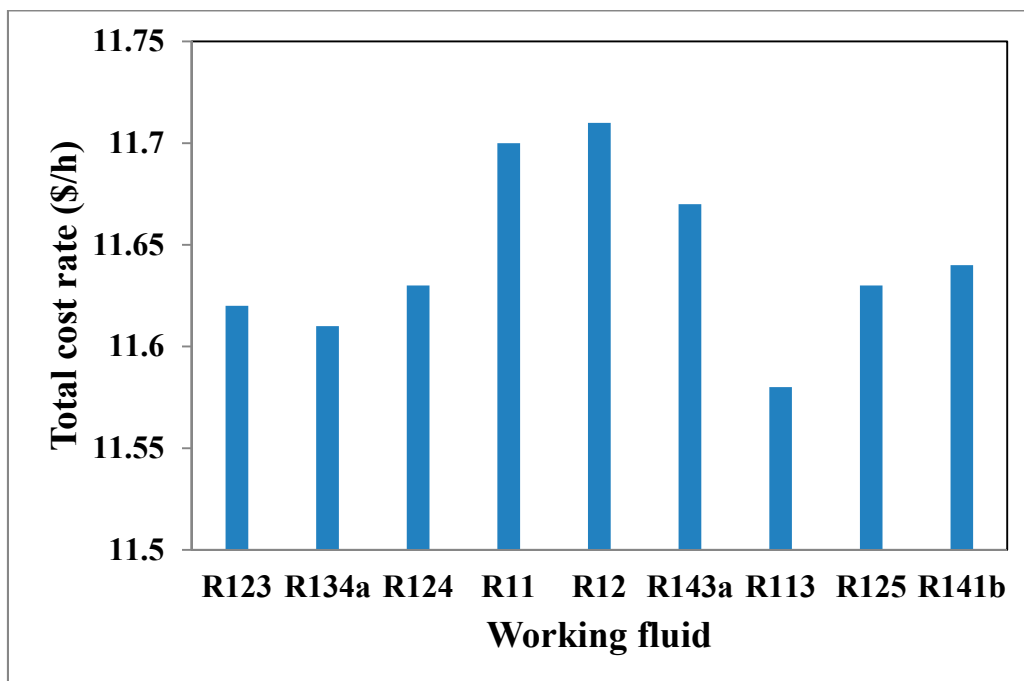
The results of the present thermodynamic analysis are presented here, including assessments of the effects of varying several design parameters on the cycle performance. As discussed earlier, the inputs of the calculation program are transferred to the present code in order to calculate the outputs. In this study the exergy efficiency, total exergy destruction and total cost rate of the CHP system are calculated for different working fluids. Figure 3 shows the exergy efficiency of different working fluids. This figure shows that R12 has the highest exergy efficiency compared to other working fluids followed by R11 and R143a. In addition, when normal boiling temperature for the working fluid decreases, the maximum pressure of the cycle should be increased to ensure saturated state at evaporator outlet. This increase in pressure usually results in higher efficiency. However, if volatility of the fluid increases, the condenser pressure must also rise significantly. Therefore, for R125 and R143a, efficiency is lower than R11 and R12.

Figure 3. Exergy efficiency of the CHP system for different working fluids.



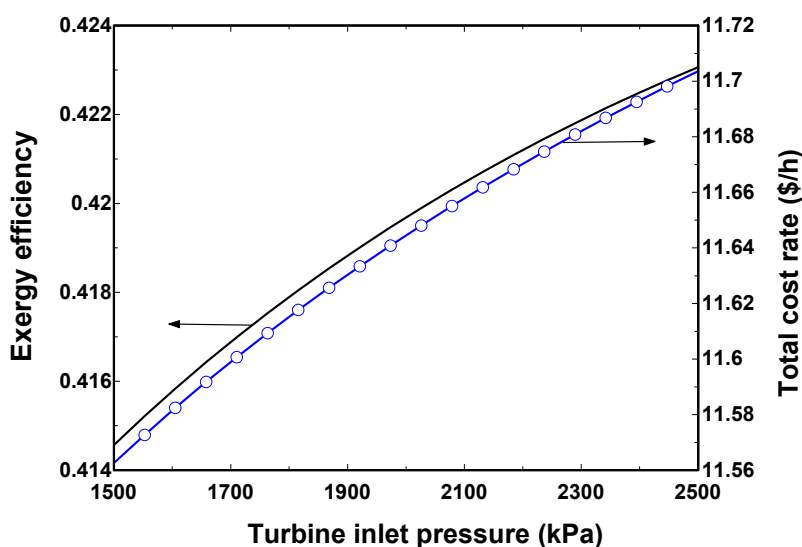
In order to enhance the understanding of the study, total cost rate of the system is also determined for different working fluids. The results are shown in Figure 4. This figure shows that R12 has the highest total cost rate among other working fluids. It was already concluded that R12 has the greatest exergy efficiency compared to other working fluids which indicates that this working fluid is good when only considering the exergy efficiency. The mass flow rate for fluids with lower normal boiling point and lower latent heat is generally higher which also increases the overall cost. Therefore, the cost rate will follow a similar trend as efficiency in Figure 3. However, from these two figures, it is concluded that R123 has a reasonable exergy efficiency while its total cost rate is lower than other working fluids except for R113, however R113 has the lowest exergy efficiency among the selected working fluids.

Figure 4. Total cost rate of the CHP system for different working fluid.



According to these results R123 is selected for the parametric study in order to see the effect of certain design parameters on the system performance. The design parameters considered here are turbine inlet pressure, condenser pressure, partial load and diesel engine nominal power. Figure 5 shows the variation of exergy efficiency and total cost rate of the CHP system with turbine inlet pressure. It is shown that an increase in turbine inlet pressure results in an increase in exergy efficiency of the system. This observation is due to the fact that the enthalpy drop across the turbine increases as the pressure ratio increases.

Figure 5. Variation with turbine inlet pressure of the exergy efficiency and total cost rate of the system.



According to the definition of exergy efficiency for this CHP system given in Equation (15) and keeping other parameters fixed, an increase in turbine inlet pressure increases the turbine work which is based on increase in turbine inlet enthalpy. Figure 5 also shows the effect of turbine inlet pressure on the

total cost rate of the system. As it is shown, an increase in turbine inlet pressure results in an increase in total cost rate of the system. As already explained, an increase in this pressure increases the turbine work and as the purchase cost of turbine is a direct function of turbine work, and increase in work results in an increase in purchase cost of the turbine which consequently increase the total cost rate of the system.

The effect of turbine inlet pressure on total exergy destruction rate of the system is shown in Figure 6. It shows that an increase in turbine inlet pressure decreases the total exergy destruction rate of the system, due mainly to an increase in turbine work. According to the exergy balance equation for a control volume around the turbine, an increase in turbine work leads to a decrease in the exergy destruction rate for the turbine resulting in a reduction of total exergy destruction rate of the CHP system. Therefore the higher the turbine inlet pressure the higher the exergy efficiency and the lower the total exergy destruction rate. Figure 7 confirms this trend and indicates that an increase in turbine inlet pressure increases the net output power as discussed earlier, and also an increase in turbine inlet pressure decreases the normalized CO₂ emission of the system again according to an increase in net output power. As the mass flow rate into the diesel engine is fixed, an increase in net output power with the same amount of fuel results in a reduction of normalized CO₂ emission of the system.

Another important parameter in power generation cycles is condenser pressure which strongly affects the performance of the system. Figure 8 shows the effect of condenser pressure on both exergy efficiency and total cost rate of the system. It is shown that an increase in condenser pressure decrease the exergy efficiency of the CHP system. An increase in condenser pressure increases the heat rejected to the environment which increases the enthalpy at Point 5 in Figure 1. Thus, an increase in this enthalpy results in an increase in condenser heat rejection of the system and an increase in enthalpy at Point 5 decreases the turbine work which finally decreases the net output power of the CHP system. As it is shown in Figure 8, an increase in condenser pressure decreases the total cost rate of the system, due to a decrease in both turbine work and condenser heat transfer area. Therefore, an increase in condenser pressure has a negative effect on system exergy efficiency while having a positive effect on total cost rate of the system. Thus this parameter is a good parameter for the optimization study that will be presented afterward.

Figure 6. Variation with turbine inlet pressure of the exergy efficiency and total exergy destruction rate.

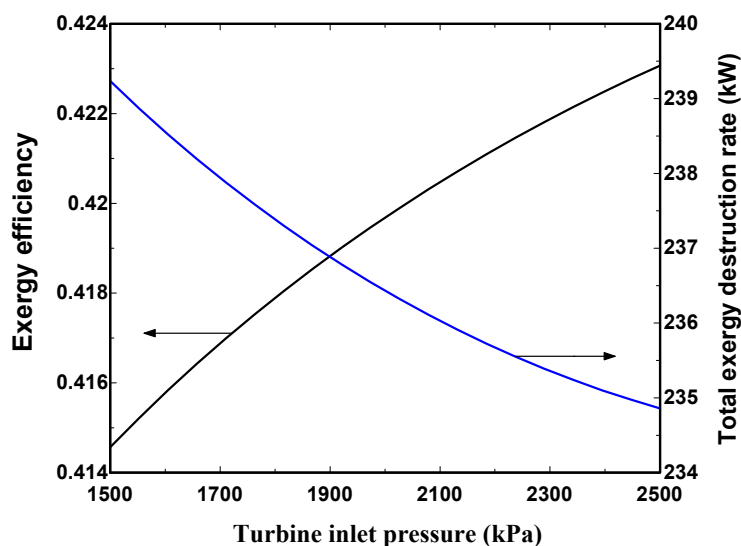


Figure 7. Variation with turbine inlet pressure of the output power and normalized CO₂ emission.

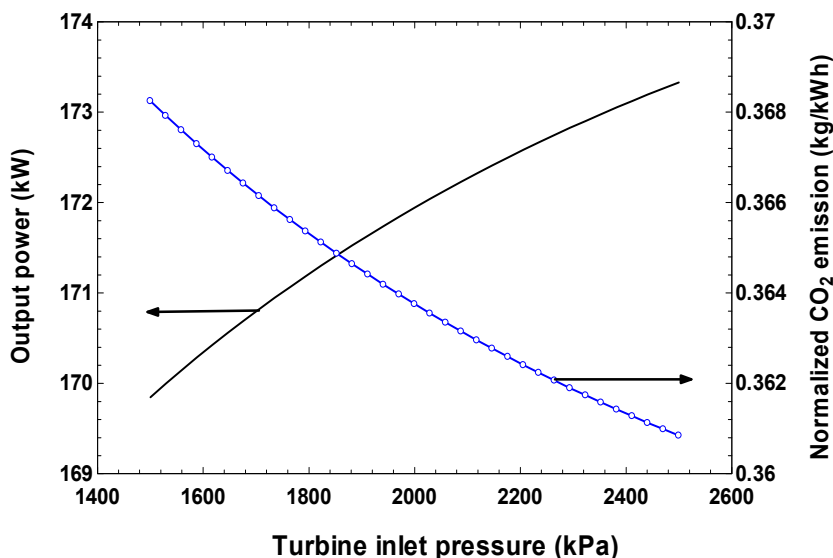


Figure 8. Variation with condenser pressure of the exergy efficiency and total cost rate of the system.

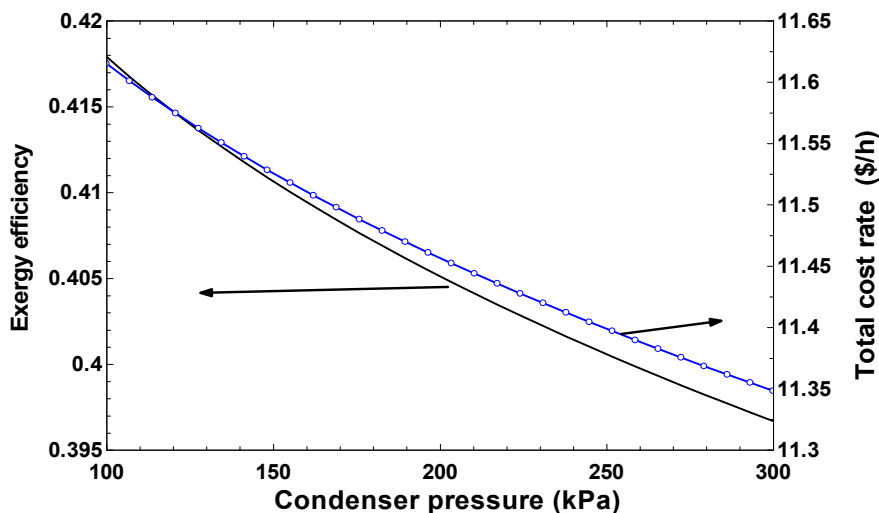
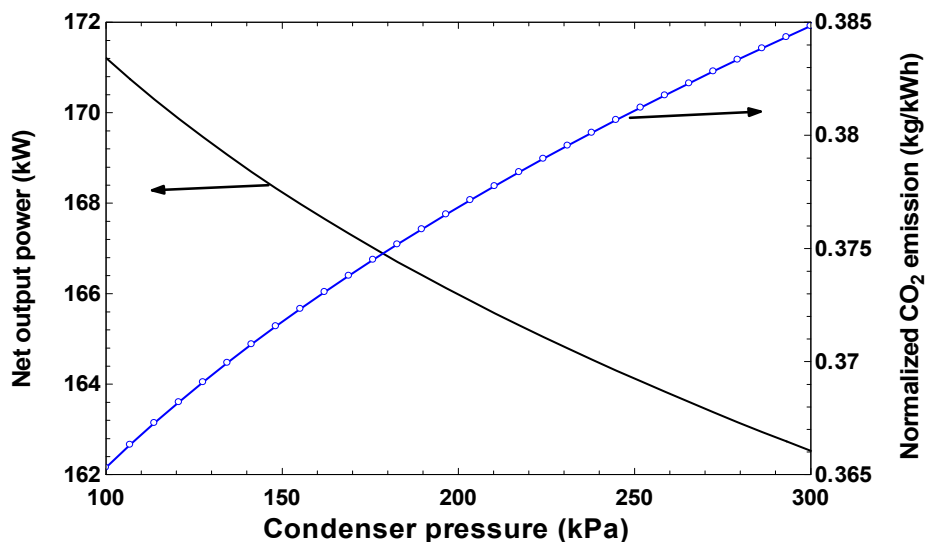


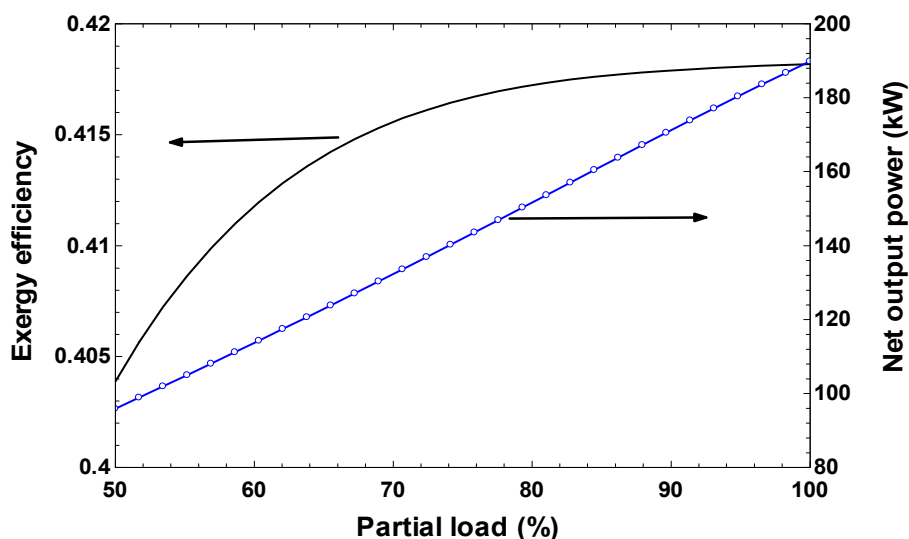
Figure 9 shows the effect of condenser pressure on both net output power and normalized CO₂ emission of the CHP system. As shown in this figure an increase in condenser pressure decreases the net output power, mainly due to an increase in ORC turbine outlet enthalpy which results in a decrease in turbine work and increase in heat rejected to the environment. In addition, it is seen that an increase in condenser pressure increases the normalized CO₂ emission of the system. Since the fuel mass flow rate into the diesel engine is constant, a decrease in net output power leads to an increase in CO₂ emission of the system.

Figure 9. Variation with condenser pressure of the net output power and normalized CO₂ emission.



Partial load of the diesel engine is another important factor that affects the system performance. Figure 10 shows the effect of partial load on system exergy efficiency and net output power. It is shown that an increase in partial load increases both system exergy efficiency and net output power. This is due to the fact that an increase in diesel engine load results in an increase in mass flow rate injected to the engine, which eventually leads to an increase output power. Also, it increases the heat to the ORC cycle which results in an increase in ORC turbine work. This is the main reason that an increase in diesel engine load increases both net power and exergy efficiency.

Figure 10. Variation with partial load of the exergy efficiency and net output power.



The effect of partial load on normalized CO₂ emission and total exergy destruction rate of the system is shown in Figure 11. As shown here, an increase in partial load decreases the normalized CO₂ emission of the system due to several effects. As already explained, an increase in partial load results in an increase in mass flow rate injected into the diesel engine and increases the net output power. However, the increase in output power dominates, eventually leading to a decrease in CO₂ emission of the system. In

addition, an increase in this parameter increases the total exergy destruction rate of the CHP system which is due to an increase in exergy destruction rate of the diesel engine. This increase is due to an increase in fuel exergy which is the input exergy flow of the diesel engine.

Figure 11. Variation with partial load of the normalized CO₂ emission and total exergy destruction rate.

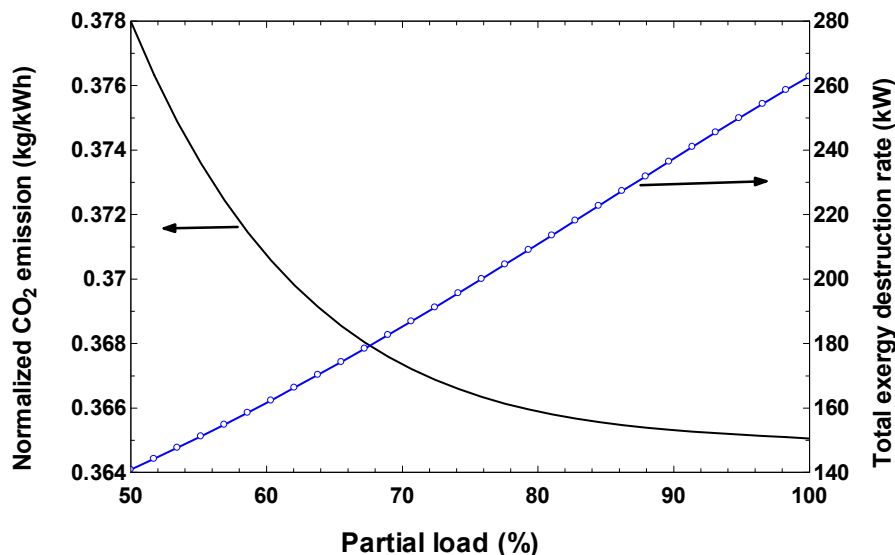
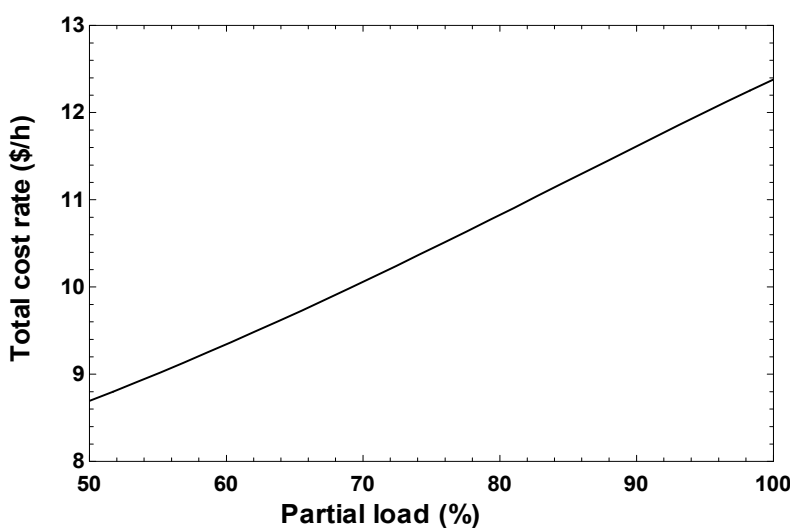


Figure 12 shows the effect of partial load of the diesel engine on the total cost rate of the system. As shown, an increase in partial load of the diesel engine increases the total cost rate of the system. This is due to an increase in fuel cost and ORC turbine purchase cost which leads to an increase in total cost of the system.

Figure 12. Variation with partial load of the total cost rate of the system.



6.3. Multi-Objective Optimization Results

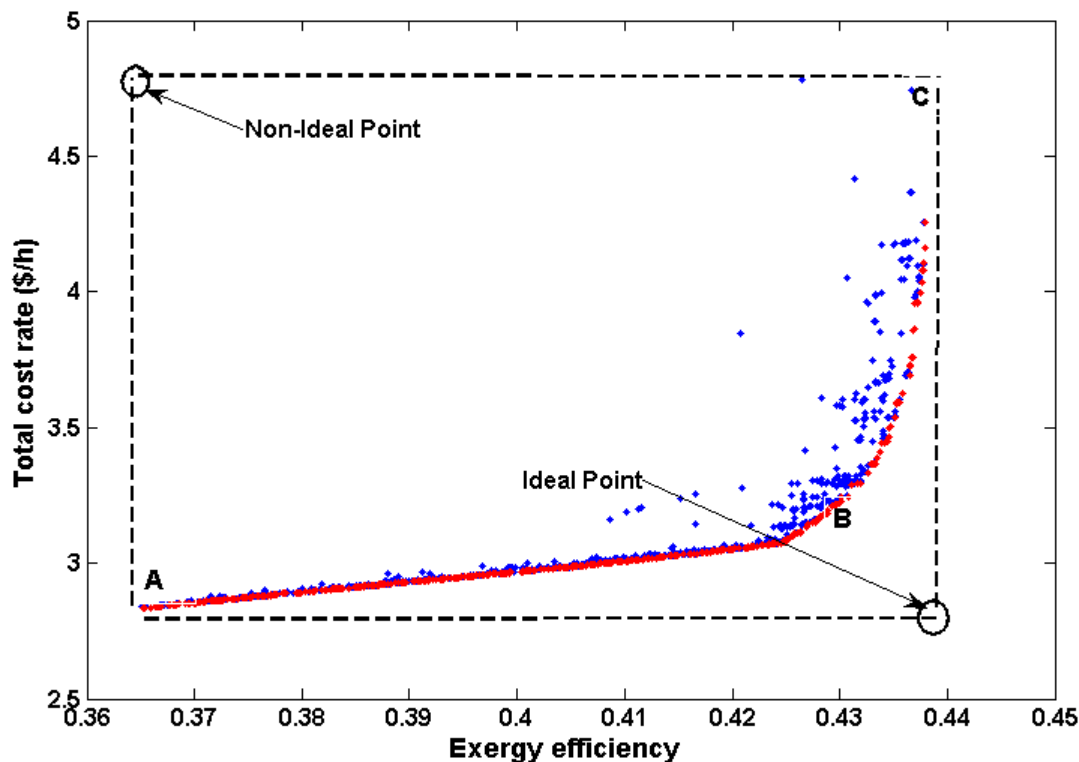
In this section, the optimization results are presented in more detail. Figure 13 shows the Pareto frontier solution for this multi-generation system with objective functions given in Equations (16) and (17) in multi-objective optimization. This figure shows the total cost rate of products increases moderately as the total exergy efficiency of the cycle increases to approximately 41%. By increasing the total exergy efficiency from 41% to 44%, the cost rate of the products increases significantly. As shown in Figure 13, the maximum exergy efficiency is illustrated at design point *C* (43.86%), while the total cost rate of products is also the best at this point (4.73 \$/h). At design point *A*, however, the minimum value for the total cost rate of product occurs (about 2.72 \$/h). When efficiency is the sole objective function, the design point *C* is the optimal situation, however when total cost rate of product is the sole objective function, design point *A* is the optimum point. Pareto frontier contains the best solution family of the problem. Selecting the best point is not a clear and general approach and is dependent on the procedure of decision making and changing parameters. A more general approach is using the concept of equilibrium point, which is the intersection of the asymptotic surface of the Pareto frontier.

In this regard, a set of asymptotics are plotted for each Pareto frontier and their intersection shows the equilibrium point. Thus, the best solution is the point which has the minimum distance from the equilibrium point. In addition, the procedure of calculating the equilibrium point and minimum distance point is a fully automatic approach which is programmed and applied to all cases. In this regard, Figure 13 point *B* is the ideal point in which both objectives have their optimal values independent of the other objectives. Nevertheless, in this case, the Pareto optimum frontier exhibits weak equilibrium, *i.e.*, a small change in exergy efficiency from varying the operating parameters causes a large variation in the total cost rate of product. Therefore, the equilibrium point cannot be utilized for decision making in this problem. In selection of the final optimum point, it is desired to achieve a better magnitude for each objective than its initial value for the base case problem. Therefore, the optimized points in the *B-A* region have the maximum exergy efficiency increment of approximately 3% and minimum total cost rate increment of approximately 1.5 \$/h relative to design point *B*, and thus design point *B* can be a good candidate for the multi-objective optimization.

Note that in multi-objective optimization and the Pareto solution, each point can be utilized as the optimized point. Therefore, the selection of the optimum solution depends on the preferences and criteria of the decision maker, suggesting that each may select a different point as the optimum solution depending on the decision maker's needs. Table 5 lists all the design parameters for points *A*, *B* and *C*. To assist with optimal design of the multi-generation system, the following expression (valid in the range of $36\% < \psi < 44\%$) is derived for the Pareto optimal points curve (as shown in Figure 13):

$$\dot{C}_{tot} = \frac{-21.54\psi^2 + 7.4\psi + 10.95}{\psi^4 - 8.29\psi^3 + 10.1\psi^2 - 17.37\psi + 9.4} \quad (18)$$

Figure 13. Pareto frontier: best trade off values for the objective functions.



The thermodynamic characteristics of three different points on the Pareto frontier are listed in Table 6 and show the selection of each point on the Pareto curve.

Table 5. Optimized decision variables for selected points on Pareto frontier.

Point	\dot{W}_{nom} (kW)	PL (%)	P_4 (kPa)	P_5 (kPa)	$\eta_{Turbine}$ (-)	η_{Pump} (-)
A	50	50.07	1004	28,843	0.7541	0.80
B	50	50	2496	63	0.9	0.84
C	54.76	99	2491	50.5	0.9	0.8612

Table 6. Thermodynamic characteristics of three different points on the Pareto frontier.

Point	\dot{W}_{net} (kW)	Ψ (%)	$\dot{Ex}_{D,tot}$ (kW)	$\dot{CO}_{2,dim}$ (kW)	\dot{C}_{tot} (\$/h)
A	28.87	0.3635	45.99	0.42	2.827
B	32.55	0.425	45.06	0.3592	3.074
C	70.28	0.4423	91.71	0.3451	4.72

7. Conclusions

A diesel engine CHP system is developed in this research study, and the effect of different working fluids on the performance assessment of the system is assessed. It was concluded that R123 has the better performance assessment compared to other working fluids. Exergy analysis confirms that the diesel engine for waste heat recovery can increase the exergy efficiency of the system by approximately 45%. A calculus-based optimization approach using evolutionary algorithms (*i.e.*, genetic algorithms) allows multi-objective optimization of the multi-generation plant. Some other concluding remarks follow:

- An increase in ORC turbine inlet pressure leads to an increase in exergy efficiency of the system
- An increase in turbine inlet pressure has a negative effect on the total cost rate of the system
- An increase in condenser pressure decreases the exergy efficiency of the system while having a positive effect on the total cost rate of the system
- An increase in partial load of the diesel engine increases exergy efficiency of the system, net output power and the total cost rate of the system, and decreases the normalized CO₂ emission of the system

Acknowledgments

The authors would like to thank to Ministry of Science, Technology and Innovation (MOSTI) (Sciencefund 4S046) as well as the Ministry of Education Malaysia (MOE), and Research Management Centre (RMC), Universiti Teknologi Malaysia (GUP 01G60) for awarding a research grant to undertake this project.

Author Contributions

The contributions of each author are as follows: Abdolsaeid Ganjehkaviri provided the impetus for this work and analyzed the numerical results and drafted the manuscript. Mohammad Nazri Mohd Jaafar provided insights that led to highlighting some of the distinctions between equations and worked on rewrites and clarifications. Both authors have read and approved the final manuscript.

Conflicts of Interest

The authors declare no conflict of interest.

Nomenclature

C	Total cost rate, (\$/h)
ex	specific exergy, (kJ/kg)
$\dot{E}x_D$	exergy destruction rate, (kW)
h	specific enthalpy, (kJ/kg)
LHV	lower heating value, (kJ/kg)
\dot{m}	mass flow rate, (kg/s)
P	pressure, (kPa)
PL	partial load (%)
\dot{Q}	heat transfer rate, (kW)
R	gas constant, (kJ/kg K)
s	specific entropy, (kJ/kg K)
T	temperature, (°C)
\dot{W}	work rate, (kW)

\dot{Z}_k purchase cost of each component

Greek Letters

η_{Pump} pump isentropic efficiency, (%)

η_T turbine isentropic efficiency, (%)

Ψ exergy efficiency, (%)

Subscripts

act actual

Cond condenser

Die diesel

e outlet condition

env environmental

f fuel

HEX heat exchanger

i inlet condition

is isentropic

mix mixture

nom nominal

oil oil

ph physical

prim

P pump

T turbine

tot total

wj water jacket

0 reference environment condition

Superscripts

Ch chemical

. rate

References

1. Teng, H.; Regner, G.; Cowland, C. *Waste Heat Recovery of Heavy-Duty Diesel Engines by Organic Rankine Cycle Part I: Hybrid Energy System of Diesel and Rankine Engines*; SAE Technical Paper No. 2007-01-0537; SAE International: Warrendale, PA, USA, 2007; doi:10.4271/2007-01-0537.
2. Teng, H.; Regner, G.; Cowland, C. *Waste Heat Recovery of Heavy-Duty Diesel Engines by Organic Rankine Cycle Part II: Workingfluids for WHR-ORC*; SAE Technical Paper No. 2007-01-0543; SAE International: Warrendale, PA, USA, 2007; doi:10.4271/2007-01-0543.
3. Ehyaei, M.A.; Ahmadi, P.; Atabi, F.; Heibati, M.R.; Khorshidvand, M. Feasibility study of applying internal combustion engines in residential buildings by exergy, economic and environmental analysis. *Energy Build.* **2012**, *55*, 405–413.
4. Dai, Y.; Wang, J.; Gao, L. Parametric optimization and comparative study of organic Rankine cycle (ORC) for low grade waste heat recovery. *Energy Convers. Manag.* **2009**, *50*, 576–582.
5. El Chammas, R.; Clodic, D. *Combined Cycle for Hybrid Vehicles*; SAE Technical Paper No. 2005-01-1171; SAE International: Warrendale, PA, USA, 2005; doi:10.4271/2005-01-1171.
6. Liu, B.T.; Chien, K.H.; Wang, C.C. Effect of working fluids on Organic Rankine Cycle for waste heat recovery. *Energy* **2004**, *29*, 1207–1217.
7. Mago, P.J.; Charma, L.M.; Srinivasan, K.; Somayaji, C. An examination of regenerative organic Rankine cycles using dry fluids. *Appl. Therm. Eng.* **2008**, *28*, 998–1007.
8. Miazza, V.; Miazza, A. Unconventional working fluids in Organic Rankine cycles for waste heat recovery systems. *Appl. Therm. Eng.* **2001**, *21*, 381–390.
9. Hajabdollahi, Z.; Hajabdollahi, F.; Tehrani, M.; Hajabdollahi, H. Thermo-economic environmental optimization of Organic Rankine Cycle for diesel waste heat recovery. *Energy* **2013**, *63*, 142–151.
10. Drescher, U.; Brüggermann, D. Fluid selection for the Organic Rankine cycle (ORC) in biomass power and heat plants. *Appl. Therm. Eng.* **2007**, *27*, 223–228.
11. Wei, D.; Lu, X.; Lu, Z.; Gu, J. Dynamic modeling and simulation of an Organic Rankine Cycle system for waste heat recovery (ORC). *Appl. Therm. Eng.* **2008**, *28*, 1216–1224.
12. San, J.Y. Second-law performance of heat exchangers for waste heat recovery. *Energy* **2010**, *35*, 1936–1945.
13. Saleh, B.; Koglbauer, G.; Wendland, M.; Fischer, J. Working fluids for low-temperature organic Rankine cycles. *Energy* **2007**, *32*, 1210–1221.
14. Roy, J.P.; Mishra, M.K.; Misra, A. Parametric optimization and performance analysis of a waste heat recovery system using Organic Rankine Cycle. *Energy* **2010**, *35*, 5049–5062.
15. Aljundi, I.H. Effect of dry hydrocarbons and critical point temperature on the efficiencies of organic Rankine cycle. *Renew. Energy* **2011**, *36*, 1196–1202.
16. Papadopoulos, A.I.; Stijepovic, M.; Linke, P. On the systematic design and selection of optimal working fluids for Organic Rankine Cycles. *Appl. Therm. Eng.* **2010**, *30*, 760–769.
17. Wakui, T.; Yokoyama, R. Optimal sizing of residential gas engine cogeneration system for power interchange operation from energy-saving viewpoint. *Energy* **2011**, *36*, 3816–3824.

18. Alanne, K.; Söderholm, N.; Sirén, K.; Beausoleil-Morrison, I. Techno-economic assessment and optimization of stirling engine micro-cogeneration systems in residential buildings. *Energy Convers. Manag.* **2010**, *51*, 2635–2646.
19. Ren, H.; Gao, W. Economic and environmental evaluation of micro CHP systems with different operating modes for residential buildings in Japan. *Energy Build.* **2010**, *42*, 853–861.
20. Aussant, C.D.; Fung, A.S.; Ugursal, V.I.; Taherian, H. Residential application of internal combustion engine based cogeneration in cold climate—Canada. *Energy Build.* **2009**, *41*, 1288–1298.
21. Garcia-Cascales, J.R.; Vera-Garcia, F.; Gonzalez-Macia, J.; Corberan-Salvador, J.M.; Johnson, M.W.; Kohler, G.T. Compact heat exchangers modeling: Condensation. *Int. J. Refrig.* **2010**, *33*, 135–147.
22. Jung, H.C.; Krumdieck, S. Modelling of organic Rankine cycle system and heat exchanger components. *Int. J. Sustain. Energy.* **2014**, *33*, 704–721.
23. Kotas, T.J. *The Exergy Method of Thermal Plant Analysis*; Butterworths: London, UK, 1985; p. 344.
24. Ganjehkaviri, A.; Mohd Jaffar, M.N.; Tholudin, M.L.; Sharifishourabi, G. Modelling and exergoeconomic based design optimisation of combined power plants. *Int. J. Exergy* **2013**, *13*, 141–158.
25. Bejan, A.; Tsatsaronis, G.; Moran, M. *Thermal Design and Optimization*; Wiley: New York, NY, USA, 1996.
26. Ganjehkaviri, A.; Mohd Jaafar, M.N.; Ahmadi, P.; Barzegaravval, H. Modelling and optimization of combined cycle power plant based on exergoeconomic and environmental analyses. *Appl. Therm. Eng.* **2014**, *67*, 566–578.
27. Bernow, S.S.; Marron, D.B. Valuation of Environmental Externalities for Energy Planning and Operations: May 1990 Update; Tellus Institute: Boston, MA, USA, 1990.
28. Bohi, D.R.; Toman, M.A. *An Assessment of Energy Security Externalities*; Discussion Paper ENR92-05; Resources for the Future: Washington, DC, USA, February 1992.
29. Ghaffarizadeh, A.; Ahmadi, K.; Flann, N.S. Sorting unsigned permutations by reversals using multi-objective evolutionary algorithms with variable size individuals. In Proceedings of 2011 IEEE congress on evolutionary computation (CEC), New Orleans, LA, USA, 5–8 Jun 2011; pp. 292–295.
30. Srinivas, N.; Deb, K. Multi-objective optimization using nondominated sorting in genetic algorithms. *Evol. Comput.* **1994**, *2*, 221–248.